Available online at www.sciencedirect.com
ScienceDirect
Geochimica et Cosmochimica Acta 71 (2007) 4942–4953
Geochimica et Cosmochimica Acta
www.elsevier.com/locate/gca

Zinc complexation in aqueous sulfide solutions: Determination of the stoichiometry and stability of complexes via $ZnS_{(cr)}$ solubility measurements at 100 °C and 150 bars

B.R. Tagirov [a,b,*], O.M. Suleimenov [a], T.M. Seward [a]

[a] *Institute for Mineralogy and Petrography, ETH Zurich, Universitaetstrasse 16, CH 8092 Zurich, Switzerland*
[b] *IGEM RAS, Staromonetnyi per. 35, 119017 Moscow, Russia*

Received 4 October 2006; accepted in revised form 14 August 2007; available online 14 September 2007

Abstract

The solubility of $ZnS_{(cr)}$ was measured at 100 °C, 150 bars in sulfide solutions as a function of sulfur concentration ($m(S_{total}) = 0.02$–0.15) and acidity ($pH_t = 2$–11). The experiments were conducted using a Ti flow-through hydrothermal reactor enabling the sampling of large volumes of solutions at experimental conditions, with the subsequent concentration and determination of trace quantities of Zn. Prior to the experiments, a long-term *in situ* conditioning of the solid phase was performed in order to attain the reproducible Zn concentrations (i.e. solubilities). The $ZnS_{(cr)}$ solubility product was monitored in the course of the experiment. The following species were found to account for Zn speciation in solution: Zn^{2+} ($pH_t < 3$), $Zn(HS)_2^0$ (pH_t 3–4.5), $Zn(HS)_3^-$ (pH_t 5–8), and $ZnS(HS)^-$ ($pH_t > 8$) (pH_t predominance regions are given for $m(S_{total}) = 0.1$). Solubility data collected in this study at $pH_t > 3$ were combined with the $ZnS_{(cr)}$ solubility product determined at lower pH to yield the following equilibrium constants ($t = 100$ °C, $P = 150$ bars):

$$Zn^{2+} + 2HS^- = Zn(HS)_2{}^0{}_{(aq)} \qquad \log\beta_2 = 9.52 \pm 0.06,$$
$$Zn^{2+} + 3HS^- = Zn(HS)_3{}^- \qquad \log\beta_3 = 12.39 \pm 0.06,$$
$$Zn^{2+} + 2HS^- = ZnS(HS)^- + H^+ \qquad \log\beta_{11} = 2.92 \pm 0.06.$$

The solubilities of $ZnS_{(cr)}$, determined beyond the Zn^{2+} predominance region (at $pH_t > 2.5$), are lower than the sphalerite solubilities previously reported in the literature, resulting in lower values of the formation constants for the Zn–S–HS complexes. The results of this study indicate that in natural sulfide-rich fluids the maximum Zn concentrations are attained at $pH = pK_1(H_2S)$, where $Zn(HS)_3^-$ predominates.

1. INTRODUCTION

Previous studies of zinc complexing in sulfide solutions made use of solubility (Glixelli, 1907; Moser and Behr, 1924; Barnes, 1959a,b, 1960a,b; Vucotic, 1961; Romberger and Barnes, 1963; Hinners and Holland, 1963; Gubeli and Ste-Marie, 1967; Melent'yev et al., 1969; Barrett and Anderson, 1982; Bourcier and Barnes, 1987; Hayashi et al., 1990; Daskalakis and Helz, 1993), voltammetry (Zhang and Millero, 1994; Luther et al., 1996, 1999), and EXAFS (Helz et al., 1993) in attempts to obtain insight into sulfide/hydrosulfide complexing of zinc. Unfortunately, these studies are not in good agreement with one another, with many conflicting stoichiometries for various proposed species (Table 1). Fig. 1 shows the solubility of sphalerite (β-ZnS, the low-temperature polymorph of zinc sulfide) as a function of pH calculated using literature data from which thermodynamic functions

* Corresponding author. Address: IGEM RAS, Staromonetnyi per. 35, 119017 Moscow, Russia.
E-mail address: tagir@igem.ru (B.R. Tagirov).

0016-7037/$ - see front matter © 2007 Elsevier Ltd. All rights reserved.
doi:10.1016/j.gca.2007.08.012

Table 1
Experimental studies of the Zn–S–H_2O system available from the literature

System composition	Method	t (°C)	pH	$m(S_{total})$	Species, concentrations	Reference
ZnS–H_2O–H_2S–H_2SO_4	Solubility of ZnS precipitated with H_2S from aqueous solutions of Zn salts. Solid phases were not characterized	20, 25	0.001–1 m H_2SO_4	2.4×10^{-5}–0.1	Zn^{2+}	Glixelli (1907), Moser and Behr (1924). Compiled by Ravitz (1936)
ZnS–H_2O–H_2S	Solubility of sphalerite. The solid phase was prepared by precipitation with H_2S from Zn acetate or chloride solution at ambient temperature, dried during 8 h at 120 °C, and recrystallized in H_2S atmosphere during 250 h at 135–150 °C	50–200	~3	Solutions saturated with $H_2S_{(l)}$, $m(S) = 1.5$ (50 °C)–3.5 (200 °C)	$Zn(HS)_2^0$	Vucotic (1961), experimental data reduction performed by Khodakovsky (1966)
ZnS–H_2O–H_2S–($HClO_4$ or NaOH)	Solubility of ZnS was measured using radioactive indicator technique. Solid phase was not characterized	25	0.75–13.4	4×10^{-4}–0.01	Zn^{2+}, $Zn(HS)OH^0$	Gubeli and Ste-Marie (1967)
ZnS–H_2O–H_2S–NaCl–(HCl or NaOH)	Solubility of sphalerite was measured using radioactive indicator technique. Solid phase was prepared by reaction of $ZnCl_2$ with H_2S at 25–600 °C	100–180	$pH_{25°}$ 0.6–8	0.1 to ~0.85	Zn^{2+}, $Zn(HS)_2^0$, $Zn(HS)_3^-$ or $ZnHS_2^-$	Melent'yev et al. (1969)
ZnS–H_2S and ZnS–H_2S–H_2O	Solubility of natural coarse-grained sphalerite was measured in pure liquid H_2S, liquid H_2S saturated with H_2O, and H_2O equilibrated with gaseous H_2S. Solutions were sampled at experimental conditions	25–180	2.9–4 (aqueous phase)		Zn concentration in the aqueous phase was close to the background (~1 mg/L), in pure H_2S was <0.1 mg/L, but increased to ~11 mg/L in H_2S liquid saturated with water	Barnes (1959a,b)
ZnS–H_2O–H_2S–NaOH and ZnS–H_2S–H_2O–S	Solubility of natural coarse-grained sphalerite was determined in aqueous H_2S–NaOH solutions, in pure H_2S_x liquids, H_2O saturated H_2S_x liquid, and in the aqueous phase coexisting with H_2S_x liquid	To 200	4–8.2 (aqueous phase)		$ZnHS_2^-$ in aqueous NaHS solutions. In pure H_2S_x liquids, H_2O saturated H_2S_x liquid, and in the aqueous phase coexisting with H_2S_x liquid, C(Zn) was below the detection limit (~50 mg/L)	Barnes (1960a,b)
ZnS–H_2O–H_2S–NaOH	Solubility of sphalerite	25–200	8.06			Romberger and Barnes (1963)
ZnS–H_2O–H_2S–NaCl–(NaOH or HCl)	Solubility pf sphalerite in NaCl solutions (m(NaCl) = 0–4).	80	1.5–6.5	H_2S-saturated solutions	Zn-Cl complexes, ZnS·H_2S, ZnS·HS^-	Hinners and Holland (1963)
ZnS–H_2O–H_2S–NaCl–(NaOH or HCl)	Solubility of natural Santandar sphalerite	27–95	0.8–7	0.02–0.3	Zn^{2+}, Zn-Cl species $Zn(HS)_2^0$, $Zn(HS)_2^-$	Barrett and Anderson (1982)
ZnS–H_2O–H_2S–NaOH	Solubility of natural Santandar sphalerite	100–350	6.1–9.6	0.1–2.3	$Zn(OH)(HS)^0$, $Zn(HS)_2^0$, $Zn(HS)_3^-$, $Zn(HS)_4^{2-}$	Bourcier and Barnes (1987)
ZnS–H_2O–H_2S–NaOH	Solubility of synthetic sphalerite	25–240	3.3–11	0.5–2.4	$Zn(HS)_2^0$, $Zn(HS)_4^{2-}$, $Zn(HS)_3^-$, $Zn(OH)(HS)_2^-$, $Zn(OH)(HS)_3^{2-}$	Hayashi et al. (1990)

(*continued on next page*)

Table 1 (*continued*)

System composition	Method	t (°C)	pH	$m(S_{total})$	Species, concentrations	Reference
ZnS–H_2O–H_2S–(NaOH or HCl)	Solubility of synthetic and natural sphalerite	25	2.2–9.1	0.0004–0.1	Zn^{2+}, Zn–Cl species, $Zn(HS)_2^0$, $ZnS(HS)_2^{2-}$; $Zn(HS)_4^{2-}$, $ZnHS_2^-$	Daskalakis and Helz (1993)
ZnS (sphalerite or amorphous)–H_2O–H_2S	EXAFS	25	9.4	9	Not specified	Helz et al. (1993)
Zn in seawater + H_2S	Voltammetry	25	8	10^{-9}–10^{-6}	$ZnHS^+$, $Zn(HS)_2^0$	Zhang and Millero (1993)
Zn in seawater + H_2S	Voltammetry	25	2–8	10^{-3}–1.5×10^{-2}	ZnS^0, $Zn_2S_3^{2-}$	Luther et al. (1996)
Zn in seawater + H_2S	Voltammetry, UV–vis spectroscopy, filtration	25	7–8.3	10^{-3}–1.5×10^{-2}	$Zn_3S_3^0$, $Zn_4S_6^{4-}$	Luther et al. (1999)

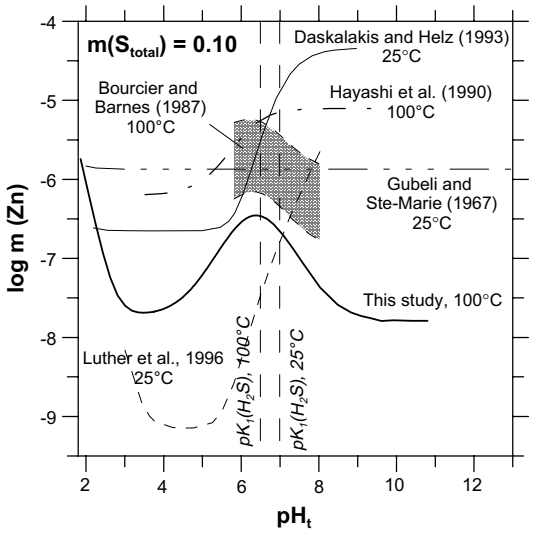

Fig. 1. Logarithm of Zn concentration in equilibrium with $ZnS_{(cr)}$ as a function of pH for total sulfur concentration 0.1 m (results of this study compared with the sphalerite solubility according to literature data). The stability constants of $ZnS^0_{(aq)}$ and $Zn_2S_3^{2-}$ reported by Luther et al. (1996) were combined with $\Delta_f G^o_{(298.15K)}(Zn^{2+})$ and $\Delta_f G^o_{(298.15K)}(ZnS_{(cr)})$ from Wesolowski et al. (1998) and Robie and Hemingway (1995), respectively, to yield the sphalerite solubility curve. $\Delta G^o_T(ZnS_{(cr)})$ from Robie and Hemingway (1995) was used to calculate the solubility curves using data of Bourcier and Barnes (1987) and Hayashi et al. (1990). For other studies, the sphalerite solubility product determined by the authors was used.

pertaining to sphalerite dissolution at temperatures from 25 to 100 °C for $m(S_{total}) = 0.1$ could be derived. The literature data presented in Table 1 and shown in Fig. 1 are inconsistent in terms of Zn concentration in equilibrium with sphalerite as well as regarding Zn speciation. Gubeli and Ste-Marie (1967) have found out that the ZnS solubility decreased with increasing pH at pH 0.75–3 (Zn^{2+} predominates), but pH and $m(S_{total})$ independent at pH > 3 because of $Zn(HS)OH^0_{(aq)}$ formation. Bourcier and Barnes (1987) determined that the predominant Zn complex is $Zn(HS)_3^-$, whose stability decreases with increasing temperature, whereas $Zn(HS)_2{}^0{}_{aq}$ and $Zn(HS)_4^{2-}$ become predominant at high temperatures ($t > 250$ °C). In contrast, Hayashi et al. (1990) suggested that Zn–HS complexes predominate in acidic solutions, but mixed Zn–HS–OH species dominate Zn speciation at alkaline pH. This speciation model yields higher sphalerite solubility in alkaline solutions than models without hydroxide–hydrosulfide complexes (Fig. 1). Daskalakis and Helz (1993) developed speciation model which was similar to that of Hayashi et al. (1990) at alkaline pH, but Daskalakis and Helz (1993) did not observe $Zn(HS)_3^-$ in acidic solutions. The disagreements amongst the literature data on sphalerite solubility is due to a number of effects which may include the degree of sphalerite crystallinity, grain size, uncertainties of analytical methods and, probably, sphalerite stoichiometry, bearing in mind that sphalerite may be a zinc deficient phase, as was noted by Scott and Barnes (1973). Zhang and Millero (1994) and Luther et al. (1996) studied the zinc speciation in seawater in the presence of H_2S using voltammetry, but the speciation models developed by these authors are different (Table 1). The sphalerite solubility curve calculated using the ZnS^0 and ZnS_3^{2-} stability constants from Luther et al. (1996) does not agree with the results of solubility determinations mentioned above (Fig. 1).

In hydrothermal fluids in the Earth's crust, zinc is transported mainly in the form of chloride and hydrosulfide complexes (Barnes and Czamanske, 1967). Khodakovsky (1966) compiled the sphalerite solubility data available from the literature and suggested that, in the geologically important pH range from 1.5 to ~8 in the presence of H_2S, the predominant Zn species are Zn^{2+}, $Zn(HS)_2^0$, and $Zn(HS)_3^-$. Barnes (1960b) and later Khodakovsky (1966) have determined that the stability of Zn–HS complexes is almost independent of temperature, and therefore, oxidation, loss of H_2S and pH change may cause changes in the dissolved Zn speciation and be the main factors controlling Zn deposition from hydrothermal ore solutions. These observations were consistent with more recent experimental studies (c.f. Hayashi et al., 1990). Accordingly, the knowledge of the stoichiometry of hydrosulfide and sulfide complexes of Zn is necessary for accurate modelling of its hydrothermal transport and deposition.

In this study, the stoichiometry and stability of Zn species dominating in sulfide solutions were determined at 100 °C and 150 bars, $m(S_{total}) = 0.02$–0.15, and pH_t 2–11 (pH_t corresponds to the experimental temperature)

from the $ZnS_{(cr)}$ solubility measurements with the use of a flow-through hydrothermal reactor. Similar experimental designs were used at our laboratory in studies of the Cu–H_2S–H_2O and Ag–H_2S–H_2O systems (Mountain and Seward, 2003, and Stefánsson and Seward, 2003, respectively). The experimental parameters were chosen because reconnaissance experiments showed that, at $t < 100$ °C, the Zn concentrations at the minima of the solubility curve were quite low (i.e. $<1 \times 10^{-8}$ m), and hence, the measured solubilities involved large analytical uncertainties, which prevented the reliable determination of the stoichiometry and stability of the predominant complexes. The flow-through experimental solubility technique made it possible to sample large volumes of experimental solutions and, after concentrating, to accurately enough determine trace quantities of Zn. Using this advantage of the flow-through technique, the stoichiometries of Zn complexes predominating at the minima of the solubility curve, at which the metal concentrations are low (~0.1 ppb of Zn at $m(S_{total}) \sim 0.1$), were determined. A long-term conditioning of the solid phase before the start of the solubility experiments was carried out, and the $ZnS_{(cr)}$ solubility product was monitored in the course of the experiments. Therefore, in this study not only the $ZnS_{(cr)}$ solubility constants but also the stability constants for Zn hydrosulfide/sulfide complexes were calculated directly from the experimental solubility data by combining the solubility constants with the solubility product obtained for the solid phase.

2. EXPERIMENTAL

The $ZnS_{(cr)}$ solubility measurements were performed using a flow-through reactor (Fig. 2). Experimental solutions were prepared by mixing two stock solutions: H_2S-saturated water (flask 1, delivered to pump 1), and NaOH, $HClO_4$ or H_2O (flask 2, delivered to pump 2). The glass flasks were hermetically closed and pressurized with ~0.7 bar (above atmospheric pressure) of Ar grade 6.0 (>99.9999 vol %) or H_2S grade 2.0 (≥99.0 vol %). The overpressure was necessary to prevent the formation of gas bubbles in the pump head. The solutions were delivered via Teflon tubing to HPLC pumps fitted with Ti heads. The wetted parts of the pump heads were Ti, a sapphire piston, a high-density polyethylene seal ring and hasteloy C spring inside the seal ring. The pumps were connected, via 1/16 inch PEEK tubing, to a PEEK column with an internal volume of ~5 ml, which served as a mixing reservoir. After the column, the solution was either passed through a Ti valve into a pH cell (described below) and to the waste flask or was delivered via Ti grade 2 tubing (0.25 in. OD, 0.1 in. ID) into the reactor (all fittings were made of Ti Grade 2 or Grade 5). The tubing was ~1 m long, so that the solution was preheated before entering the reactor. The reactor body was made up of a Ti–Pd alloy Ti/0.5%Pd (grade 7), with 2 μm Ti filter frits installed at both ends of the reactor. The reactor was 30 cm long and 5 cm in diameter, with an internal bore 0.8 cm in diameter tightly packed with $ZnS_{(cr)}$. The reactor was compressed with an external steel

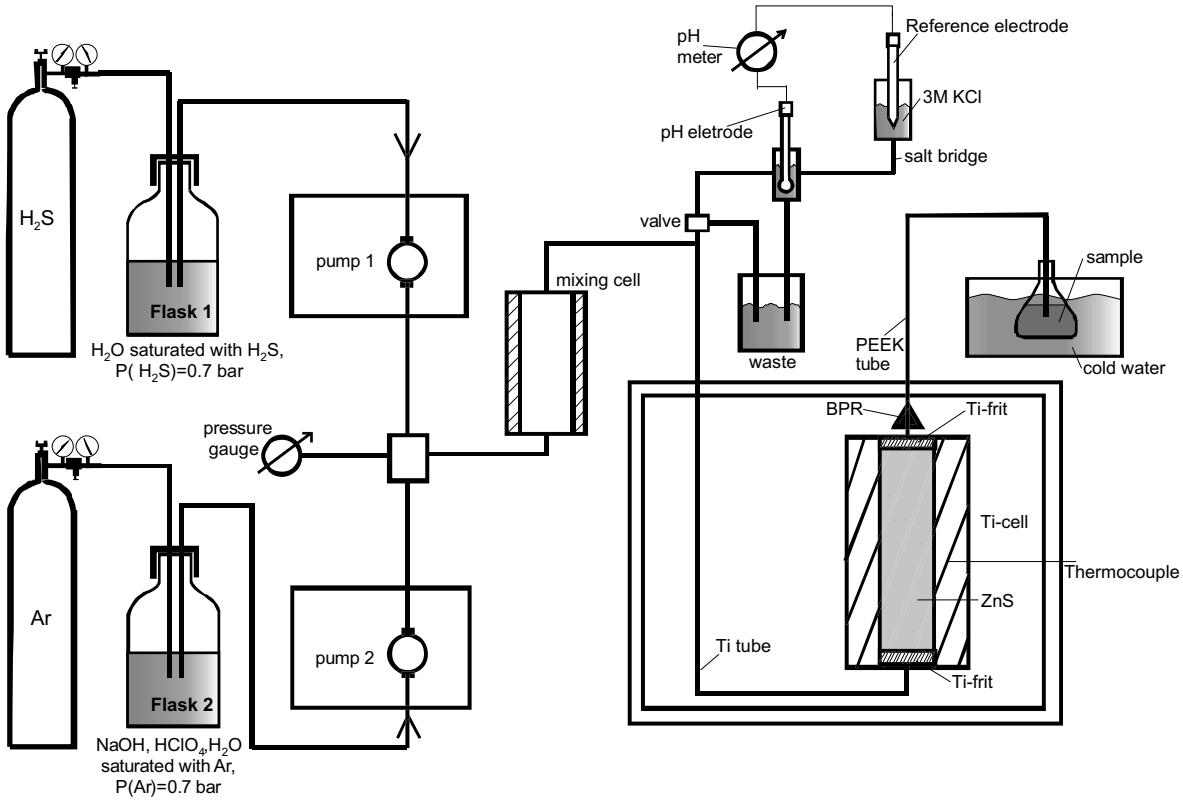

Fig. 2. Experimental facility used in the experiments.

gasket 10 cm OD. The outlet of the reactor was connected via Ti 1/16 inch tubing to CORETEST Ti back—pressure regulator with a Teflon membrane (BPR in Fig. 2). After passing through the back pressure regulator, the sampling solution flowed into a glass flask cooled with water. The pressure was monitored accurate to ±1 bar using an HPLC pump pressure transducer calibrated against an external pressure gauge. During the experiment, the pressure inside the experimental system was maintained at 150 ± 15 bars. The temperature was maintained within ±1 °C and measured using calibrated K-type thermocouple.

ZnS pieces (99.9% Aldrich) were used as a starting material. This material consisted of aggregates of fine ZnS powder. The XRD pattern of this commercial ZnS corresponded to pure sphalerite (JCPDS card 5-566). This starting material was ground and placed into silica glass ampoules together with several pieces of 99.99% sulfur (Merck) (~5 g of ZnS and ~5 mg of S). The tube with solid phases was evacuated for several minutes at slow heating (below the $S_{(cr)}$ melting point) and then sealed. The ampoules were heated in a furnace to 850 °C and kept at this temperature for 3 weeks. After this period of time, the furnace was switched off and the ampoules were allowed to cool down in the furnace. The excess sulfur crystallized on the free (not filled with ZnS) end of the ampoule during cooling. In comparison with the starting material, the recrystallized product was coarser-grained and consisted of crystalline grains ~0.1 mm across. Finally, the powder was washed several times with deionized water until the supernatant became clear and dried at 60 °C for several days. The XRD pattern of this product corresponded to pure sphalerite.

Water provided by a MilliQ system and analytical-grade chemical reagents were used throughout this study. The water used to prepare experimental solutions was boiled under vacuum in an ultrasonic bath for ~30 min and then saturated with grade 4.6 Ar passed through Cu filings heated to 425 °C in order to remove the traces of oxygen. This procedure was repeated 3 times. Concentrated 60 and 70% $HClO_4$ and 50% NaOH solutions used to prepare the experimental solutions were saturated with grade 4.6 Ar. The water used for saturating with H_2S was transferred into a 2-L bottle (flask 1 in Fig. 1) and sparged with grade 6.0 Ar for 1 h. Then the water was bubbled under stirring with H_2S for ~1–1.5 h. Prior to this, H_2S was passed through a flask with water and then through an empty flask. Finally, the outlet valve in the bottle cap was closed, the bottle was connected directly to the H_2S cylinder via a pressure reducer and pressurized with ~0.7 bar of H_2S until the total sulfur concentration become constant (~0.15 m). The water or solutions of $HClO_4$ and NaOH which were kept in another bottle (flask 2, $V = 1$ L, Fig. 1), were sparged with deoxygenated Ar for at least 30 min and then pressurized with the same gas.

Typically, 100–550 ml of solution were collected for analysis, acidified to pH 1.5–2 with concentrated HCl, and then slowly (without boiling) evaporated to dryness on a heated sand bath. The dry residues were dissolved in 4 ml of aqua regia added to the flasks, and then the aqua regia was slowly evaporated until the volume of the solution was reduced to ~0.3 ml, and finally diluted with ~5 ml of 1.5% HNO_3. The total reduced sulfur concentration was determined by iodimetric back titration with sodium thiosulphate. The Zn and Na concentrations were analyzed by flame atomic absorption spectroscopy using a Varian Spectr AA-800 spectrometer. For Na, 0.1 M HNO_3 was used as the matrix. The samples were diluted with 0.1 M HNO_3 to fall within the 1.5–3 ppm Na concentration range. The precision of the analyses was ±1% at a 95% confidence level. For Zn, the matrix was 0.5% HNO_3 + 1.5% HCl (+NaCl for alkaline samples). The concentration of acid in the range 0–3% did not affect the measured signal. Matrix matched samples containing up to 2 M of NaCl were used for the analyses. The precision of the analyses was ±3% at a 95% confidence level. The detection limit ($3\sigma_n$ of background) for Zn was 0.01 ppm. The Zn concentration in blank solutions, prepared by the same method as the samples, was below this detection limit. Standard solutions containing known Zn concentrations, as well as $HClO_4$, NaOH, and H_2S, were also treated with the above procedure without any Zn loss detected.

The pH of acid solutions was measured at room temperature (24 ± 2 °C) and ambient pressure in a flow-through micro cell, made up of a pH glass electrode and an Ag, AgCl/3 M KCl reference electrode. The pH electrode was sealed inside the test compartment of the cell (made of PVC) with a rubber o-ring. The test and reference electrodes were connected by a salt bridge (3 M KCl solution). A PEEK filter was fitted inside the test compartment at the end of the salt bridge to allow a very slow flow of the KCl solution into the test half-cell in order to eliminate the liquid junction potential. Due to the double-junction design, the length of the salt bridge (~0.5 m), and the large volume of the reference electrode compartment, the reference electrode was not contaminated with H_2S. The potentiometric cell was standardized on the activity scale using NBS standards (pH 1.68 and 4.006 at 25 °C). The accuracy of measurements was ±0.03 pH unit (determined using multiple measurements of a pH standard during a day). The determined pH values were used to calculate the concentration of $HClO_4$ and pH_t of acidic solutions.

3. DATA TREATMENT

The standard state for a pure solid phase and H_2O corresponds to a unit activity of the pure phase at a given temperature and pressure. The standard state adopted for aqueous species is unit activity for a hypothetical one molal ideal solution. The activity coefficients of charged aqueous species were calculated using the modified Debye–Hückel equation of Helgeson (1969), the ion size parameter $\mathring{a}$ was taken to be 4.5 Å for all species. For neutral species, it was assumed that $\log\gamma_n = -\log(1 + 0.018 \cdot m^*)$, where m^* is the sum of the concentrations of all solute species. The speciation calculations were performed with the help of GIBBS computer code of the HCh software package (Shvarov, 1999; Shvarov and Bastrakov, 1999). H_2O and NaOH ion pair constants were taken from Marshall and Frank (1981) and Ho et al. (2000), respectively. For NaHS, the

ion pair constant of NaCl determined by Ho et al. (1994) was used. H_2S dissociation constant was taken from Suleimenov and Seward (1997). Concentration of $ZnOH^+$, $ZnOH_2{}^0{}_{(aq)}$, and $ZnOH_3{}^-$ was estimated using data of Bénézeth et al. (2002). As some of the above mentioned thermodynamic constants are available only for water vapor saturated pressure (P_{sat}), all thermodynamic values used were for P_{sat}, and the pressure during thermodynamic calculations was set at P_{sat}.

The Gibbs free energies for Zn–S–HS species were calculated by two methods. First, the calculation was performed with the aid of the GIBBS computer code by manual iteration to match the observed solubilities. Second, these values were refined via minimizing the objective function $F = \sum \left(m(\mathrm{Zn})_{\mathrm{measured}} - m(\mathrm{Zn})_{\mathrm{calculated}}\right)^2$ by means of the Levenberg–Marquardt technique (Levenberg, 1944; Marquardt, 1963). The minimizing procedure was carried out in the Matlab 7.1. computational language with the $m(\mathrm{Zn})_{\mathrm{calculated}}$ values computed using the GIBBS computer code. Calls to the external Gibbs free energy minimization routine (GIBBS computer code) were realized through the ActiveX component GibbsLib.dll. The convergence was assumed to be achieved when the F function values for two subsequent cycles differed by less than 10^{-4}% of the measured concentration.

The variances of the optimized Gibbs free energies were estimated from the Hessian of $F(x)$, calculated at the solution (Bard, 1974). The confidence interval was calculated at a 95% confidence level. Finally, the optimized values of the Gibbs free energies for Zn–S–HS complexes were recalculated, together with the corresponding confidence intervals, into the logarithms of the reaction constants as $\log K = -\Delta_r G/(2.303 \cdot \mathrm{RT})$.

The solubility of a fresh batch of synthetic $ZnS_{(cr)}$, which had been annealed either dry or in contact with solution, decreased slowly with time. This solubility decrease took place continuously during one month of the reconnaissance experiments at 25–75 °C and precluded accurate determining the solubility constants. In order to attain a stable solubility product value, a batch of $ZnS_{(cr)}$ was conditioned *in situ* at 250 °C in contact with approximately 25 L of 0.1 m sulfide solution at pH 2–8 for 2 months. After this treatment, the measured Zn concentrations (i.e. solubilities) stabilized and the main experimental series was started. The XRD analysis performed on a sample of $ZnS_{(cr)}$ after the experiments did not show any significant change relative to the initial product. Moreover, a similar solubility decrease was observed for some other batches of synthetic $ZnS_{(cr)}$, as well as for natural Santandar sphalerite. Therefore, we suggest that the possible reason for the solubility decrease could be the dissolution (i.e. elimination) of small particles of the solid phase or surface defects (etches, sharp angles etc.). The attainment of equilibrium Zn concentrations was checked by performing solubility experiments at pH 2 at flow rates of 0.5–8 ml/min. The measured Zn concentration was independent of the flow rate, which means that the stationary $ZnS_{(cr)}$ solubility was attained. The results of our $ZnS_{(cr)}$ solubility measurements are listed in Appendix A. The equilibrium solubility constants (last four columns in Appendix A) were calculated from the Zn concentrations measured at flow rates of 1.5–4 ml/min and were also found to be independent of the flow rate. The calculated concentration of Zn hydroxide complexes was always lower than 10^{-11} m (less than 1% of total Zn concentration). Fig. 3 shows the solubility of $ZnS_{(cr)}$ as a function of pH at $m(\mathrm{S_{total}}) = 0.1$. Points represent the experimental solubility data recalculated for $m_{\mathrm{S_{total}}} = 0.1$ using the Zn speciation model given below. The solid line corresponds to Zn concentrations calculated using the solubility constants determined in this study. The solubility curve showed in Fig. 3 exhibits four regions with different slopes vs. pH. In acidic solutions, $\log m(\mathrm{Zn_{total}})$ decreases with increasing pH, with the maximum slope close to two, indicating that 2 mole of protons are consumed for the dissolution of one mole of $ZnS_{(cr)}$, and Zn^{2+} predominates as given by,

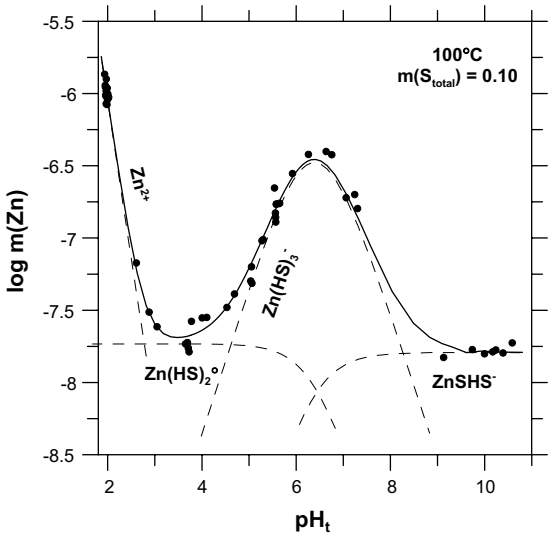

Fig. 3. Logarithm of Zn concentration in equilibrium with $ZnS_{(cr)}$ at 100 °C and $m(\mathrm{S_{total}}) = 0.1$ as a function of pH_t. Points correspond to experimental solubility data, lines are calculated using $ZnS_{(cr)}$ solubility constants from Table 2.

$$ZnS_{(cr)} + 2H^+ = Zn^{2+} + H_2S^0{}_{(aq)} \quad (1)$$

for which,

$$\log K_{s0} = \log a(H_2S^0{}_{(aq)}) + \log a(Zn^{2+}) + 2 \cdot \mathrm{pH}, \quad (1a)$$

where a is the activity of the species indicated. The stoichiometry of reaction (1) is consistent with previous studies performed in acidic media (Table 1), and was confirmed by measurements of the $ZnS_{(cr)}$ solubility as a function of $m(H_2S)$ at pH 2 performed at 25–250 °C in the reconnaissance experimental series (the slope of $\log m(\mathrm{Zn})$ vs. $\log m(H_2S)$ was close to −1 throughout the whole temperature range). Fig. 4 shows the $ZnS_{(cr)}$ solubility product (reaction 1) which was monitored in the course of the experiment. As shown in this figure, there is no systematic change in the $ZnS_{(cr)}$ solubility product. The scatter of the experimental data is mostly due to the uncertainty in calculated pH_t. The value of $\log K_{s0} = -3.276 \pm 0.022$ will be used below in order to calculate the Zn–S–HS complexes stability constants.

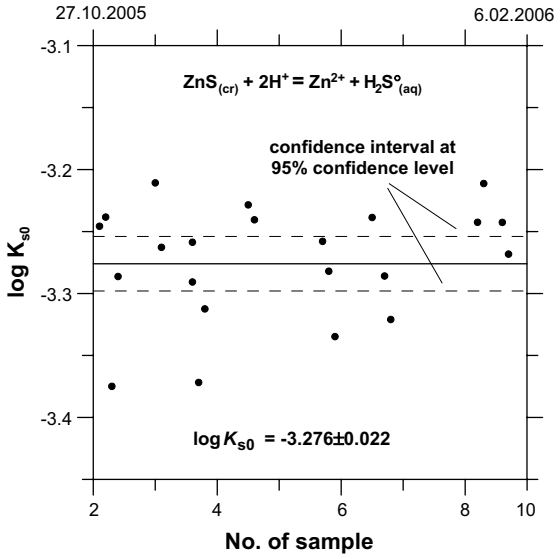

Fig. 4. Variations in the logarithm of the $ZnS_{(cr)}$ solubility product in the sampled solutions.

Between pH 3 and 4, the measured $ZnS_{(cr)}$ solubility is pH independent (Fig. 3), indicating that H^+ does not participate in $ZnS_{(cr)}$ dissolution. The slope of $\log m(\mathrm{Zn})$ vs. $\log m(\mathrm{S_{total}})$ is close to 1 (Fig. 5a), which is consistent with the reaction,

$$ZnS_{(cr)} + H_2S^0_{(aq)} = Zn(HS)_2{}^0_{(aq)} \quad (2)$$

for which,

$$\log K_{s2} = \log a(Zn(HS)_2{}^0_{(aq)}) - \log a(H_2S^0_{(aq)}). \quad (2a)$$

The further decrease in the acidity to $\mathrm{pH} = \mathrm{p}K_1(H_2S)$ results in an increase in the measured Zn concentrations, indicating that the $ZnS_{(cr)}$ dissolution takes place with the liberation of protons. The slope of $\log m(\mathrm{Zn})$ vs. $\log m(\mathrm{S_{total}})$ is close to 2 (Fig. 5b), and the $ZnS_{(cr)}$ dissolution reaction is

$$ZnS_{(cr)} + 2H_2S^0_{(aq)} = Zn(HS)_3{}^- + H^+. \quad (3)$$

At $\mathrm{pH} > \mathrm{p}K_1(H_2S)$, the decrease observed in the Zn concentration is related to a change in the predominant sulfur species. For this pH region, reaction (3) may be rewritten as

$$ZnS_{(cr)} + 2HS^- + H^+ = Zn(HS)_3{}^- \quad (4)$$

which implies that Zn concentration decreases with increasing pH. For thermodynamic calculations, it is more convenient to use the reaction

$$ZnS_{(cr)} + HS^- + H_2S^0_{(aq)} = Zn(HS)_3{}^- \quad (5)$$

$$\log K_{s3} = \log a(Zn(HS)_3{}^-) - \log a(H_2S^0_{(aq)}) - \log a(HS^-) \quad (5a)$$

such that the numbers of charged species and their charges on both sides of the reaction are equal. At pH 7.5–9, it was not possible to reliably control pH because of the proximity to the H_2S–NaOH system equivalence point. At $\mathrm{pH} > 9$, the observed solubility is pH independent (Fig. 3), whereas the

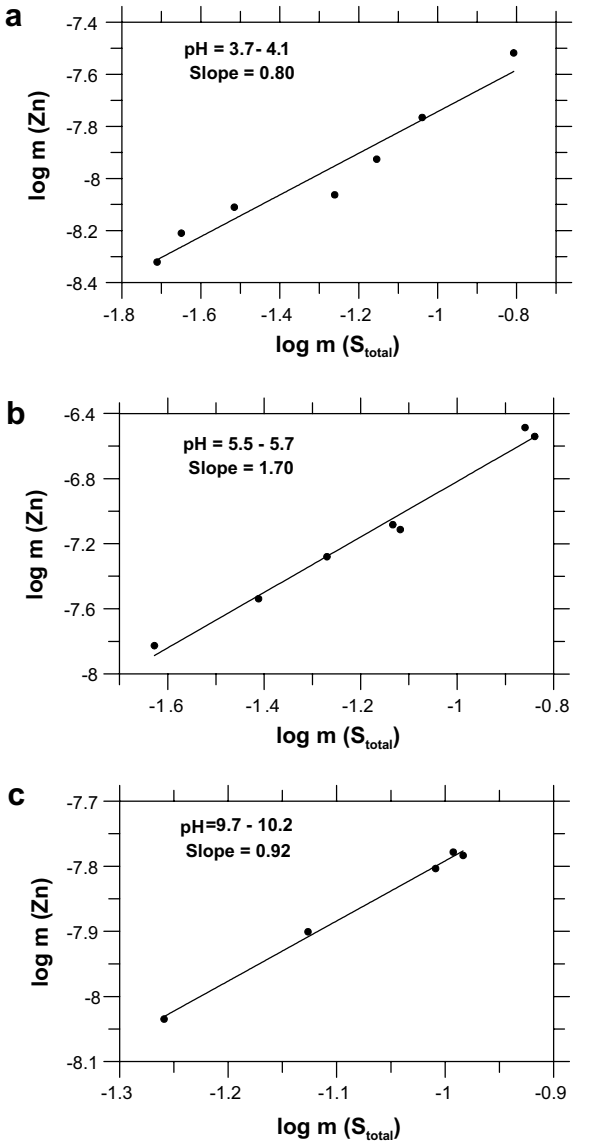

Fig. 5. Logarithm of Zn concentration in equilibrium with $ZnS_{(cr)}$ as a function of $\log m(\mathrm{S_{total}})$.

slope of $\log m(\mathrm{Zn})$ vs. $\log m(\mathrm{S_{total}})$ is close to 1 (Fig. 5c) which yields the reaction

$$ZnS_{(cr)} + HS^- = ZnS(HS)^- \quad (6)$$

$$\log K_{s11} = \log m(ZnS(HS)^-) - \log a(HS^-). \quad (6a)$$

The slopes of the solubility curves discussed above represent only approximate stoichiometries of Zn species, because (i) the pH of the experimental solutions (indicated in Fig. 5a–c) were not exactly the same, (ii) other complexes contributed to the measured solubilities, and (iii) activity coefficients were not taken into account. However, in all considered pH regions, the calculated $ZnS_{(cr)}$ solubility constants (last four columns in Appendix A) are pH and $m(\mathrm{S_{total}})$ independent, which confirms the Zn speciation model developed in this study (note that the values of the $ZnS_{(cr)}$ solubility constants listed in Appendix A are provi-

Table 2
Logarithms of the $ZnS_{(cr)}$ solubility constants (final values, calculated via least-squares regression) and stability constants for Zn–S–HS aqueous complexes

$ZnS_{(cr)} + 2H^+ = Zn^{2+} + H_2S°_{(aq)}$	$\log K_{s0} = -3.28 \pm 0.02$
$ZnS_{(cr)} + H_2S°_{(aq)} = Zn(HS)_2°$	$\log K_{s2} = -6.74 \pm 0.04$
$ZnS_{(cr)} + H_2S°_{(aq)} + HS^- = Zn(HS)_3^-$	$\log K_{s3} = -3.86 \pm 0.03$
$ZnS_{(cr)} + HS^- = ZnS(HS)^-$	$\log K_{s11} = -6.85 \pm 0.05$
$Zn^{2+} + 2HS^- = Zn(HS)_2°$	$\log \beta_2 = 9.52 \pm 0.06$
$Zn^{2+} + 3HS^- = Zn(HS)_3^-$	$\log \beta_3 = 12.39 \pm 0.06$
$Zn^{2+} + 2HS^- = ZnS(HS)^- + H^+$	$\log \beta_{11} = 2.92 \pm 0.06$

sional ones and were employed only to illustrate the plausibility of the Zn speciation model. The final values for these constants, which were refined using least-squares mathematical procedure, are listed in Table 2). Finally, we note that the solubilities measured at the minima of the solubility curve (pH 3–4 and pH > 9) were on the order of 0.1–1 ppb and, after concentrating, always 1.5–2 times exceeded the detection limit. Therefore, we believe that, even at the minima of the solubility curve, the measured Zn concentrations characterize the solubility of $ZnS_{(cr)}$, and are not at the detection limit of the analytical method, as was probably the case with some of the aforementioned studies.

Table 2 summarizes the final values of the $ZnS_{(cr)}$ solubility constants. These values are in excellent agreement with those calculated by the manual iteration of the $ZnS_{(cr)}$ solubility data (Appendix A). The maximum discrepancies between the measured and calculated solubilities were never larger than 0.16 log units (most points fall within 0.1 log units (Fig. 6), that is within the uncertainty of pH, $m(S_{total})$, and $m(Zn_{total})$ determinations), with no systematic deviations observed between the measured solubility and the calculated values. This fact also testifies for the plausibility of the Zn speciation model accepted in this study. Fig. 7 shows

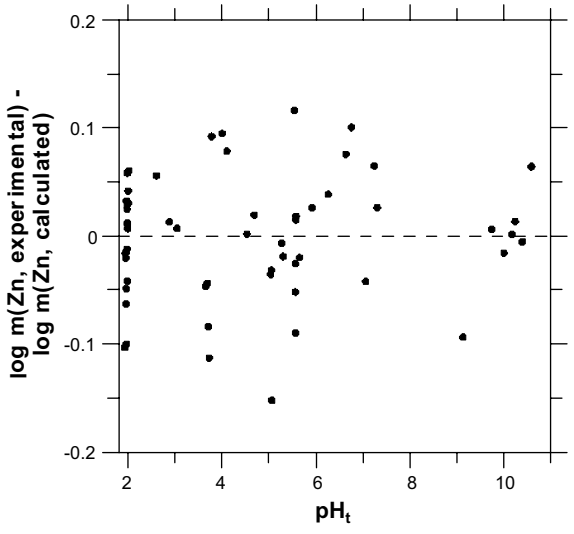

Fig. 6. Plot of the logarithm of the experimental Zn concentration minus logarithm of concentration predicted using the sphalerite solubility constants listed in Table 2 as a function of pH.

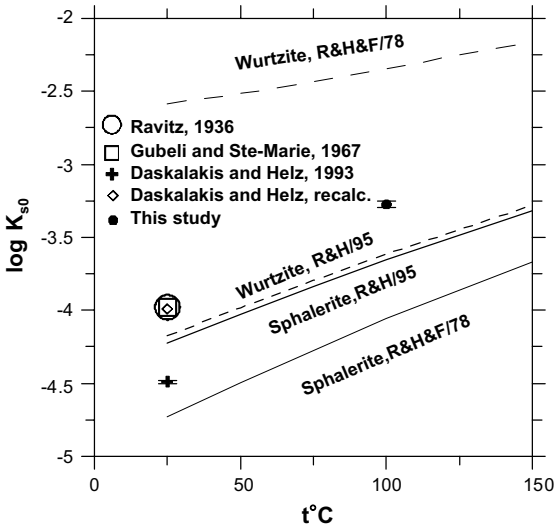

Fig. 7. Temperature function of $\log K_{s0}(ZnS_{(cr)} + 2H^+ = Zn^{2+} + H_2S°_{(aq)})$. Symbols correspond to experimental solubility data. The cross shows the original value given in Daskalakis and Helz (1993), and the diamond corresponds to the average value calculated using Daskalakis and Helz's (1993) sphalerite solubility data for pH 2.20 and 2.28, together with Zn–Cl complexes stability constants from the critical compilation of Martell et al. (1997). The lines were calculated using the thermodynamic properties of $ZnS_{(cr)}$ from Robie et al. (1978) and Robie and Hemingway (1995) (R&H&F/78 and R&H/95, respectively), zincite solubility product ($ZnO + 2H^+ = Zn^{2+} + H_2O$) from Wesolowski et al. (1998), and thermodynamic properties of zincite from Robie et al. (1978) and Kubaschewski and Alcock (1983) (for the entropy and heat capacity and for the Gibbs free energy of formation, respectively).

the temperature dependence of the sphalerite and wurtzite solubility products (equilibrium 1). The lines were calculated using the thermodynamic properties of Zn^{2+} obtained from zincite ($ZnO_{(cr)}$) solubility measurements (Wesolowski et al., 1998). The value of the equilibrium constant for zincite dissolution reaction $ZnO_{(cr)} + 2H^+ = Zn^{2+} + H_2O_{(l)}$ determined at 100 °C by Wesolowski et al. (1998) ($\log K_s = -8.12$) is in good agreement with the value calculated using the thermodynamic properties for the reaction components recommended by CODATA (1989) ($\log K_s = -8.06$). This calculated value was combined with thermodynamic properties of $ZnS_{(cr)}$ from Robie et al. (1978) and Robie and Hemingway (1995) to yield the $ZnS_{(cr)}$ solubility products. The sphalerite solubility products determined via sphalerite solubility measurements (points in Fig. 7, including $ZnS_{(cr)}$ solubility product determined in this study) are always higher than the calculated values (solid lines). Therefore, in order to eliminate the uncertainty related to the value of $\Delta_f G°(ZnS_{(cr)})$, the $ZnS_{(cr)}$ solubility constants determined here were combined with the $ZnS_{(cr)}$ solubility product and with the H_2S dissociation constant ($\log K_1(H_2S) = -6.49 \pm 0.01$, Suleimenov and Seward, 1997) to obtain equilibrium constants, β_n, for the formation of hydrosulfidozinc (II) complexes:

$$Zn^{2+} + 2HS^- = Zn(HS)_2^{0}{}_{(aq)} \quad (7)$$

$$\log \beta_2 = \log a(\mathrm{Zn(HS)_2^0{}_{(aq)}}) - 2 \cdot \log a(\mathrm{HS^-}) - \log a(\mathrm{Zn^{2+}}) \quad (7a)$$

$$\mathrm{Zn^{2+} + 3HS^- = Zn(HS)_3^-} \quad (8)$$

$$\log \beta_3 = \log a(\mathrm{Zn(HS)_3^-}) - 3 \cdot \log a(\mathrm{HS^-}) - \log a(\mathrm{Zn^{2+}}) \quad (8a)$$

$$\mathrm{Zn^{2+} + 2HS^- = ZnS(HS)^- + H^+} \quad (9)$$

$$\log \beta_{11} = \log a(\mathrm{ZnS(HS)^-}) - 2 \cdot \log a(\mathrm{HS^-}) - \mathrm{pH} - \log a(\mathrm{Zn^{2+}}). \quad (9a)$$

The derived stability constants are given in Table 2.

Fig. 1 compares the $ZnS_{(cr)}$ solubilities observed in the present study with the sphalerite solubility data available from the literature. Apart from the Zn^{2+} predominance field, the solubility curve determined in this study lies below all literature sphalerite solubility data (note that data of Luther et al. (1996) were obtained using voltammetry). The shape of the solubility curve recorded in this study and, therefore, the speciation model, are consistent with the speciation model developed in Bourcier and Barnes (1987) ($Zn(HS)_3^-$ predominates at pH 6–8). The speciation models developed in other studies of sphalerite solubility are in conflict with our results. Zhang and Millero (1994) voltammetrically determined the stability constants of $ZnHS^+$ and $Zn(HS)_2^0{}_{(aq)}$. These values are not consistent with the results of this study because (i) we did not observe the formation of $ZnHS^+$ in the experimental solutions, and (ii) the stability constant of $Zn(HS)_2^0{}_{(aq)}$, determined here ($\log \beta_2 = 9.52$, Table 2) is much lower than the value determined by these authors ($\log \beta_2^* = 13.7$ at 25 °C and ionic strength of sea water, $I = 0.7$). The shape of the sphalerite solubility curve, as well as the concentrations of Zn calculated using the formation constants for $ZnS^0{}_{(aq)}$ and ZnS_3^{2-} retrieved by Luther et al. (1996) from voltammetric experimental data, are different from those determined in the present study (Fig. 1).

4. Zn SPECIATION IN HYDROTHERMAL FLUIDS

The constants determined in the present study can be used, together with the literature data on the stability of Zn–Cl complexes to evaluate Zn speciation in hydrothermal fluids and determine the conditions of Zn ore formation. Fig. 8a and b shows predominance diagrams for Zn aqueous species in NaCl–HCl–H_2S solutions at 100 °C, P_{sat}. We assumed that mixed hydroxide chloride complexes of Zn are not important. We also suppose that, with heating, the predominance fields of Zn–Cl complexes expand at the expense of Zn–S–HS species as the stability of the former increases in high-temperature solutions, whereas the stability of Zn–S–HS complexes is only weakly sensitive to temperature (e.g. Bourcier and Barnes, 1987). As follows from these diagrams, in acidic hydrothermal solutions Zn is transported in mainly the form of chloride complexes ($ZnCl^+$ and $ZnCl_2$). With a decrease in the H_2S concentration, the predominance fields of Zn–Cl complexes expand towards higher pH (Fig. 8b). As can be seen form the sphalerite solubility curve (Fig. 3) in comparison with Fig. 8, the

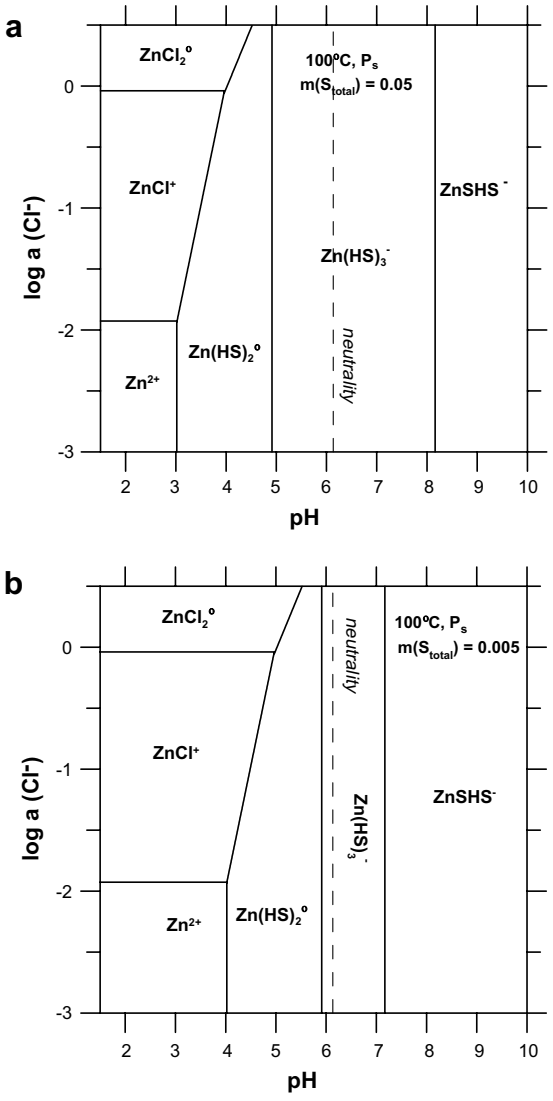

Fig. 8. Log$a(Cl^-)$ vs. pH diagram for the predominance of Zn aqueous species at 100 °C, P_{sat} and $m(S_{total}) = 0.05$ (a), and 0.005 (b). The stability of Zn–Cl complexes was calculated via regression of values from the CRITICAL database (Martell et al., 1997) for 25 °C and the data of Ruaya and Seward (1986) for higher temperatures.

concentration of dissolved Zn in acidic solutions (Zn–Cl complexes predominate) can be much higher (by a few orders of magnitude) than the concentrations at weakly acidic and alkaline pH, at which Zn–S–HS complexes predominate. Therefore, acidic chloride fluids are responsible for Zn hydrothermal transport at many hydrothermal Zn deposits, including submarine deposits in the Red Sea (Cronan, 1980), black smokers (Zierenberg et al., 1984; Grichyk, 2000; Bogdanov et al., 2006), and the low-temperature ore-forming system at the Cheleken Peninsula (Lebedev and Nikitina, 1983). The neutralization of acidic fluids results in the deposition of the bulk of Zn in the form of sphalerite. However, geological observations indicate that ore transporting fluids at some mineral deposits can be weakly acidic to near-neutral. For example, the Kuroko type (Pb–Cu–Zn)

deposits mineralized fluids were in equilibrium with montmorillonite–seritsite–quartz and K-feldspar–muscovite–quartz mineral assemblages. These equilibria yield pH within the range of 4.5–6.5 at 200–350 °C and $m(K) = 0.01–0.1$ (Ohmoto and Skinner, 1983; Franklin et al., 1981). In these fluids Zn can be transported with both Zn–Cl and $Zn(HS)_3^-$ complexes. The cooling of these fluids, together with pH change towards more alkaline values due to mixing with seawater or another solution of high pH, would result in Zn deposition because of (i) a change in the Zn predominant complex (Zn–Cl complexes in high-temperature acidic solutions, and $Zn(HS)_3^-$ and $ZnSHS^-$ at lower temperatures and alkaline pH), and (ii) a decrease in the Zn solubility because of pH shift and a change in the S predominant species (HS^- at $pH > pK_1(H_2S)$, Fig. 3) in the region of $Zn(HS)_3^-$ predominance. Analogously, pH changes may lead to Zn deposition from sulfide-rich solutions because of interaction of hydrothermal fluid with calcareous siltstones or limestone (Cu–Pb–Zn sulfide deposits in the Roudnyi Altai, eastern Kazakhstan, and southern Siberia (Bespaev et al., 1997), and sulfide deposits of the Uralian (Ci–Zn) type, Prokin and Buslaev (1999), respectively).

ACKNOWLEDGMENTS

We are grateful to E. Kurdyukov for correcting the English version of the manuscript, and to A.V. Zotov for constructive and helpful discussions in the course of the experimental study and discussion of the ms text. We are greatly indebted to I.V. Vikentyev and V.L. Rusinov for their help in the geological application of the experimental data. This research was supported by ETH and Schweizerischer Nationalfonds research funding awarded to T.M. Seward, the Russian Program for support of Leading Scientific Schools to B. Tagirov, and the European Associate Laboratory "Environmental Geochemistry" (LEAGE). We thank three anonymous reviewers for their scrupulous reviews, which helped us to improve the manuscript.

APPENDIX A

Composition of experimental solutions, calculated solute concentrations (mol/kg H_2O), and estimated values of the logarithms of the $ZnS_{(cr)}$ solubility constants. The latter values are the provisional estimates of the solubility constants (calculated by manual iteration) and were used only to demonstrate the plausibility of the speciation model.

Sample N	Experimental values				Calculated values			$\log K_s$ (Zn^{2+})	$\log K_s$ ($Zn(HS)_2°$)	$\log K_s$ ($Zn(HS)_3^-$)	$\log K_s$ ($ZnS(HS)^-$)
	m(Zn)	$m(H_2S)$	m(NaOH)	$m(HClO_4)$[a]	pH	$[HS^-]$	$[H_2S°]$				
100/1	1.45E−06	7.32E−02	0	1.200E−02	1.98	2.55E−06	7.32E−02	−3.25			
100/2	1.47E−06	7.32E−02	0	1.200E−02	1.98	2.55E−06	7.32E−02	−3.24			
100/3	1.39E−06	7.02E−02	0	1.330E−02	1.94	2.23E−06	7.02E−02	−3.37			
100/4	1.55E−06	7.22E−02	0	1.290E−02	1.95	2.36E−06	7.22E−02	−3.29			
100/5	6.17E−09	2.24E−02	0	1.258E−04	3.78	4.40E−05	2.24E−02		−6.62		
100/6	8.65E−09	5.49E−02	0	9.508E−05	3.73	9.61E−05	5.48E−02		−6.86		
100/7	1.71E−08	9.14E−02	0	6.060E−05	3.69	1.47E−04	9.13E−02		−6.78		
100/8	3.03E−08	1.56E−01	0	0	3.65	2.29E−04	1.56E−01		−6.79		
100/9	1.19E−08	7.01E−02	0	8.071E−05	3.71	1.18E−04	6.99E−02		−6.83		
100/10	1.31E−06	7.03E−02	0	1.080E−02	2.02	2.69E−06	7.03E−02	−3.21			
100/11a	1.32E−06	7.06E−02	0	1.150E−02	2.00	2.55E−06	7.06E−02	−3.26			
100/11	5.12E−08	1.33E−01	1.48E−03	0	4.53	1.51E−03	1.32E−01			−3.88	
100/12	5.95E−08	1.25E−01	2.04E−03	0	4.69	2.06E−03	1.23E−01			−3.85	
100/13	6.22E−08	7.91E−02	4.89E−03	0	5.27	4.89E−03	7.42E−02			−3.88	
100/14	6.02E−08	9.98E−02	3.63E−03	0	5.04	3.64E−03	9.62E−02			−3.92	
100/16	1.35E−06	7.18E−02	0	1.170E−02	1.99	2.56E−06	7.18E−02	−3.26			
100/17	1.25E−06	6.69E−02	0	1.230E−02	1.97	2.28E−06	6.69E−02	−3.37			
100/18	1.27E−06	6.89E−02	0	1.180E−02	1.98	2.43E−06	6.89E−02	−3.31			
100/19	1.21E−07	1.45E−01	5.55E−03	0	5.05	5.51E−03	1.40E−01			−3.91	
100/20	2.03E−07	1.48E−01	1.00E−02	0	5.30	9.99E−03	1.38E−01			−3.89	
100/21	3.41E−07	1.11E−01	2.71E−02	0	5.92	2.70E−02	8.39E−02			−3.84	
100/22	3.04E−07	8.99E−02	3.77E−02	0	6.26	3.75E−02	5.22E−02			−3.82	
100/23	1.99E−07	7.09E−02	4.50E−02	0	6.64	4.47E−02	2.59E−02			−3.77	
100/24	7.21E−08	6.01E−02	5.27E−02	0	7.24	5.23E−02	7.41E−03			−3.74	
100/25	1.47E−06	6.57E−02	0	1.130E−02	2.00	2.41E−06	6.57E−02	−3.23			
100/26	1.36E−06	6.68E−02	0	1.110E−02	2.01	2.49E−06	6.68E−02	−3.24			
100/27	4.78E−09	1.95E−02	0	0	4.10	8.01E−05	1.94E−02		−6.65		
100/29	7.76E−09	3.05E−02	0	0	4.00	1.00E−04	3.04E−02		−6.63		
100/30	5.25E−08	5.37E−02	6.39E−03	0	5.58	6.39E−03	4.73E−02			−3.84	
100/31	1.49E−08	2.36E−02	2.51E−03	0	5.54	2.51E−03	2.11E−02			−3.69	
110/32	2.89E−08	3.88E−02	4.55E−03	0	5.58	4.55E−03	3.42E−02			−3.84	
100/33	8.25E−08	7.36E−02	8.50E−03	0	5.56	8.49E−03	6.51E−02			−3.90	
100/34	2.88E−07	1.45E−01	1.75E−02	0	5.56	1.75E−02	1.28E−01			−3.93	
100/35	4.22E−07	1.07E−01	7.55E−02	0	6.76	7.47E−02	3.15E−02			−3.75	

(*continued on next page*)

Appendix A (*continued*)

Sample N	Experimental values				Calculated values			$\log K_s$ (Zn^{2+})	$\log K_s$ ($Zn(HS)_2°$)	$\log K_s$ ($Zn(HS)_3^-$)	$\log K_s$ ($ZnS(HS)^-$)
	m(Zn)	m(H_2S)	m(NaOH)	m($HClO_4$)[a]	pH	[HS^-]	[$H_2S°$]				
100/36	1.46E−07	9.90E−02	8.87E−02	0	7.30	8.76E−02	1.03E−02			−3.80	
100/37	1.39E−06	7.02E−02	0	1.170E−02	1.99	2.50E−06	7.02E−02	−3.26			
100/38	1.36E−06	7.03E−02	0	1.190E−02	1.98	2.47E−06	7.03E−02	−3.28			
100/39	1.36E−06	7.03E−02	0	1.260E−02	1.96	2.34E−06	7.03E−02	−3.33			
100/40	1.48E−08	9.91E−02	1.00E−01	0	9.13	9.76E−02	1.70E−04				−6.90
100/41	1.87E−07	1.02E−01	8.47E−02	0	7.06	8.37E−02	1.73E−02			−3.90	
100/42	3.26E−07	1.38E−01	2.00E−02	0	5.65	1.99E−02	1.18E−01			−3.89	
100/43	7.70E−08	7.62E−02	8.97E−03	0	5.57	8.96E−03	6.72E−02			−3.97	
100/44	5.98E−08	1.13E−01	4.38E−03	0	5.06	4.39E−03	1.09E−01			−4.09	
100/45	1.52E−06	7.34E−02	0	1.220E−02	1.97	2.52E−06	7.34E−02	−3.24			
100/46	1.43E−06	7.64E−02	0	1.280E−02	1.95	2.51E−06	7.64E−02	−3.29			
100/47	1.48E−06	6.90E−02	0	1.230E−02	1.97	2.65E−06	6.90E−02	−3.29			
100/48	1.42E−06	6.62E−02	0	1.230E−02	1.97	2.25E−06	6.62E−02	−3.32			
100/50	1.79E−08	9.53E−02	1.27E−01	0	10.59	9.38E−02	5.59E−06				−6.83
100/51	1.67E−08	1.02E−01	1.14E−01	0	10.17	1.01E−01	1.57E−05				−6.83
100/52	1.65E−08	1.04E−01	1.12E−01	0	10.00	1.03E−01	2.39E−05				−6.83
100/53	1.57E−08	9.80E−02	1.18E−01	0	10.39	9.66E−02	9.07E−06				−6.87
100/55	9.23E−09	5.51E−02	5.91E−02	0	9.74	5.46E−02	2.44E−05				−6.79
100/56	1.26E−08	7.48E−02	8.82E−02	0	10.24	7.39E−02	1.01E−05				−6.82
100/59	2.85E−08	1.26E−01	0	8.900E−04	3.05	4.71E−05	1.26E−01		−6.73		
100/60	6.50E−08	1.27E−01	0	2.630E−03	2.61	1.77E−05	1.27E−01		−6.61		
100/61	3.39E−08	1.27E−01	0	1.360E−03	2.88	3.25E−05	1.27E−01		−6.72		
100/62	1.47E−06	7.26E−02	0	1.200E−02	1.98	2.53E−06	7.26E−02	−3.24			
100/63	1.49E−06	7.26E−02	0	1.170E−02	1.99	2.58E−06	7.26E−02	−3.21			
100/66	3.19E−07	1.48E−01	0	8.140E−03	2.14	7.31E−06	1.48E−01	−3.24			
100/67	3.01E−07	1.48E−01	0	8.140E−03	2.14	7.31E−06	1.48E−01	−3.27			
Average								−3.27	−6.72	−3.86	−6.85
Confidence interval at 95% confidence level								0.02	0.05	0.06	0.05

[a] Evaluated using pH measured at 25 °C.

REFERENCES

Bard Y. (1974) *Nonlinear Parameter Estimation*. Academic Press, New York.

Barnes H. L. (1959a) Ore solutions: the system ZnS–H_2S–H_2O. Carnegie Institution of Washington, Year-Book N. 58 (July 1, 1958–June 30, 1959), 163–167.

Barnes H. L. (1959b) System ZnS–H_2S–H_2O. *Bull. Geol. Soc. Am.* **70**(12), 1567.

Barnes H. L. (1960a) Ore solutions. Carnegie Institution of Washington, Year-Book N. 59 (July 1, 1959 – June 30, 1960), 137–141.

Barnes H. L. (1960b) Sphalerite solubilities in sulfide solutions. *Bull. Geol. Soc. Am.* **71**(12), 1821.

Barnes H. L. and Czamanske G. K. (1967) Solubilities and transport of ore minerals. In *Geochemistry of Hydrothermal Ore Deposits* (ed. H. L. Barnes), first ed. Holt, Rinehart and Winston, New York, pp. 334–381.

Barrett T. J. and Anderson G. M. (1982) The solubility of sphalerite and galena in NaCl brines. *Econ. Geol.* **77**, 1923–1933.

Bénézeth P., Palmer D. A., Wesolowski D. J. and Xiao C. (2002) New measurements of the solubility of zinc oxide from 150 to 350 °C. *J. Sol. Chem.* **31**, 947–973.

Bespaev Kh. A., Polyansky N. V., Ganzhenko G. D., D'yachkov B. A., Evtushenko O. P., and De L. T. (1997) Geology and metallogeny of South-West Altai (within the territory of Kazakstan and China). Gylym, Almaty (in Russian).

Bogdanov Yu. A., Lisitsin A. P., Sagalevich A. M., and Gurvich E. G. (2006) Hydrothermal ore formation of the ocean floor. Nauka, Moscow (in Russian).

Bourcier W. L. and Barnes H. L. (1987) Ore solution chemistry—VII. Stabilities of chloride and bisulfide complexes of zinc to 350 °C. *Econ. Geol.* **82**, 1839–1863.

CODATA (1989) CODATA key values for thermodynamics (eds. J. D. Cox, D. D. Wagman, and V. A. Medvedev). Hemisphere, New York.

Cronan D. S. (1980) *Underwater Minerals*. Academic Press, London.

Daskalakis K. D. and Helz G. R. (1993) The solubility of sphalerite (ZnS) in sulfidic solutions at 25 °C and 1 atm pressure. *Geochim. Cosmochim. Acta* **57**, 4923–4931.

Franklin J. M., Lydon J. W. and Sangster D. F. (1981) Volcanic associated massive sulphide deposits. In *Economic Geology Seventy-Fifth Anniversary Volume* (ed. B. J. Skinner). The Economic Geology Publishing Company, pp. 485–627.

Glixelli S. (1907) Zur theorie der H_2S-fällung der metalle. Die einwirkung von schwefelwasserstoff auf zinksalze. *Zeitschrift für Anorganische und Allgemeine Chemie* **55**, 297–320.

Grichyk D. V. (2000) *Thermodynamic Models of Submarine Hydrothermal Systems*. Scientific World, Moscow (in Russian).

Gubeli A. O. and Ste-Marie J. (1967) Constantes de stabilité de thiocomplexes et produits de solubilité de sulfures de métaux. II Sulfure de zinc. *Can. J. Chem.* **45**, 2101–2108.

Hayashi K., Sugaki A. and Kitakaze A. (1990) Solubility of sphalerite in aqueous sulfide solutions at temperatures between 25 and 240 °C. *Geochim. Cosmochim. Acta* **54**, 715–725.

Helgeson H. C. (1969) Thermodynamics of hydrothermal systems at elevated temperatures and pressures. *Am. J. Sci.* **267**, 729–804.

Helz G. R., Charnock J. M., Vaughan D. J. and Garner C. D. (1993) Multinuclearity of aqueous copper and zinc bisulfide

complexes: an EXAFS investigation. *Geochim. Cosmochim. Acta* **57**, 15–25.

Hinners N. W. and Holland H. D. (1963) Solubility of sphalerite in aqueous solutions at 80 °C. *Trans. Am. Geophys. Union* **44**(1), 116.

Ho P. C., Palmer D. A. and Wood R. H. (2000) Conductivity measurements of dilute aqueous LiOH, NaOH, and KOH solutions to high temperatures and pressures using a flow-through cell. *J. Phys. Chem. B* **104**, 12084–12089.

Ho P. C., Palmer D. A. and Mesmer R. E. (1994) Electrical conductivity measurements of aqueous sodium chloride solutions to 600 °C and 300 MPa. *J. Solut. Chem.* **23**, 997–1018.

Khodakovsky I. L. (1966) On the hydrosulphide form of heavy metal transportation in hydrothermal solutions. *Geochemistry* **8**, 960–971 (in Russian).

Kubaschewski O. and Alcock C. B. (1983) *Metallurgical Thermochemistry*. Pergamon Press, Oxford.

Lebedev L. M., and Nikitina I. B. (1983) Cheleken ore forming system. Nauka, Moscow (in Russian).

Levenberg K. (1944) A method for the solution of certain problems in least squares. *Quart. Appl. Math.* **2**, 164–168.

Luther G. W., Rickard D. T., Theberge S. and Olroyd A. (1996) Determination of metal (bi)sulfide stability constants of Mn^{2+}, Fe^{2+}, Co^{2+}, Ni^{2+}, Cu^{2+}, and Zn^{2+} by voltammetric methods. *Environ. Sci. Technol.* **30**, 671–679.

Luther G. W., Theberge S. M. and Rickard D. T. (1999) Evidence for aqueous clusters as intermediates during zinc sulfide formation. *Geochim. Cosmochim. Acta* **63**, 3159–3169.

Marquardt D. (1963) An algorithm for least-squares estimation of nonlinear parameters. *SIAM J. Appl. Math.* **11**, 431–441.

Marshall W. L. and Frank E. U. (1981) Ion product of water substance, 0–1000 °C, 1–10000 bars. New international formulation and its background. *J. Phys. Chem. Ref. Data* **10**, 295–304.

Martell A. E., Smith R. M., and Motekaitis R. J. (1997) NIST standard reference database 46 version 3.0. NIST critically selected stability constants of metal complexes database, version 3.0. Texas A&M University, College Station, TX (January 1997).

Melent'yev B. N., Ivanenko V. V. and Pamfilova L. A. (1969) Solubility of some ore-forming sulfides under hydrothermal conditions. *Geochem. Int.* **6**, 416–460.

Moser L. and Behr M. (1924) Die bestimmung der metalle der schwefelammongruppe durch schwefelwasserstoff unter druck. *Zeitschrift für Anorganische und Allgemeine Chemie* **134**, 49–74.

Mountain B. W. and Seward T. M. (2003) Hydrosulfide/sulfide complexes of copper(I): experimental confirmation of the stoichiometry and stability of $Cu(HS)_2^-$ to elevated temperatures. *Geochim. Cosmochim. Acta* **67**, 3005–3014.

Ohmoto H. and Skinner B. (1983) The Kuroko and related volcanogenic massive sulfide deposits: introduction and summary of new finding. *Econ. Geol. Monogr.* **5**, 1–8.

Prokin V. A. and Buslaev F. P. (1999) Massive Copper–Zinc Sulfide Deposits in the Urals. *Ore Geol. Rev.* **14**, 1–69.

Ravitz S. F. (1936) The solubilities and free energies of some metallic sulfides. *J. Phys. Chem.* **40**, 61–70.

Robie R. A., Hemingway B. S., and Fisher J. R. (1978) Thermodynamic properties of minerals and related substances at 298.15 K and 1 bar (10^5 Pascals) pressure and at higher temperatures. U.S. Geological Survey Bulletin 1452, U.S. Government Printing Office, Washington.

Robie R. A., and Hemingway, B. S. (1995) Thermodynamic properties of minerals and related substances at 298.15 K and 1 bar (10^5 Pascals) pressure and at higher temperatures. U.S. Geological Survey Bulletin 2131, U.S. Government Printing Office, Washington.

Romberger S. B. and Barnes H. L. (1963) Sulfide solubilities in synthetic ore solutions. *Trans. Am. Geophys. Union* **44**(1), 116.

Ruaya J. R. and Seward T. M. (1986) The stability of chloro-zinc (II) complexes in hydrothermal solutions up to 350 °C. *Geochim. Cosmochim. Acta* **50**, 651–662.

Scott S. D. and Barnes H. L. (1973) Sphalerite–wurtzite equilibria and stoichiometry. *Geochim. Cosmochim. Acta* **36**, 1275–1295.

Shvarov Yu. V. (1999) Algorithmization of the numeric equilibrium modelling of dynamic geochemical processes. *Geochem. Int.* **37**, 571–576.

Shvarov Yu. V., and Bastrakov E. N. (1999) HCh: a software package for geochemical equilibrium modelling. User's Guide. Australian Geological Survey Organization, Record 1999/25 (the internet site of the program: Available from: <http://www.ga.gov.au/minerals/research/methodology/geofluids/HCh.jsp>).

Stefánsson A. and Seward T. M. (2003) Experimental determination of the stability and stoichiometry of sulphide complexes of silver(I) in hydrothermal solutions to 400 °C. *Geochim. Cosmochim. Acta* **67**, 1395–1413.

Suleimenov O. M. and Seward T. M. (1997) A spectrophotometric study of hydrogen sulphide ionisation in aqueous solutions to 350 °C. *Geochim. Cosmochim. Acta* **61**, 5187–5198.

Vucotic S. (1961) Contribution à l'étude de la solubilité de la galène, de la blende et de chalcopyrite dans l'eau en présence d'hydrogène sulfuré entre 50 et 200 °C. *Bulletin du Bureau de Recherches Géologiques et Minères N* **3**, 11–27.

Wesolowski D. J., Bénézeth P. and Palmer D. A. (1998) ZnO solubility and Zn^{2+} complexation by chloride and sulfate in acidic solutions to 290 °C with in-situ pH measurement. *Geochim. Cosmochim. Acta* **62**, 971–984.

Zhang J.-Z. and Millero F. J. (1994) Investigation of metal sulfide complexes in sea water using cathodic stripping square wave voltammetry. *Anal. Chim. Acta* **284**, 497–504.

Zierenberg R. A., Shanks, III, W. C. and Bishoff J. L. (1984) Massive sulfide deposits at 21°N East Pacific Rise: chemical composition, stable isotopes and phase equilibria. *Geol. Soc. Am. Bull.* **95**(8), 922–929.

Associate editor: Liane G. Benning